JOURNAL OF AIRCRAFT
Vol. 48, No. 4, July–August 2011

Analytical Modeling of Runway Stone Lofting

Sang N. Nguyen* and Emile S. Greenhalgh†
Imperial College London, London, England SW7 2AZ, United Kingdom
and
Robin Olsson‡
Swerea SICOMP AB, 431 22 Mölndal, Sweden

DOI: 10.2514/1.C031306

This investigation aims to develop a closed-form analytical model to understand and predict runway stone lofting processes by considering the rigid-body interaction of a tire partially rolling over a stone. Any leading-edge aircraft structures impinging into the path of such stones could experience impacts at speeds up to the aircraft takeoff velocity, despite being some distance from the sides of the wheels. The results of the analytical model provide upper-bound envelopes of the vertical loft speeds obtained in previous numerical simulations and modified drop-weight experiments. Parametric studies conclude that the vertical loft speeds rise with increasing stone–tire overlap, stone size, and aircraft speed and with deceasing tire diameter. The outcomes of this model form a basis for vehicle designers to assess the runway stone impact threat by better understanding the physics of lofting.

Nomenclature

b = horizontal offset distance between stone and tire centers, m
C_D = aerodynamic drag coefficient
d = horizontal distance between center of stone and tip of asperity, m
e = energetic coefficient of restitution
e_g = coefficient of restitution between the stone and the ground
e_t = coefficient of restitution between the tire and the stone
F = friction force, N
F_D = aerodynamic drag force, N
g = gravitational constant, m/s^2
h = height of impact point or contact point C above ground, m
K = constant
L = length of tire footprint, m
l = overlap between the edge of the tire and the stone, % of stone diameter
m_s = mass of stone or sphere, kg
m_t = mass of tire, kg
p = height of asperity, m
q = vertical displacement of stone, m
R_c = tire cross-sectional radius, m
r = radius of stone or sphere, m
s = displacement of stone, m
t = time, s
u = vertical launch velocity of stone, m/s
V = aircraft speed relative to the ground, m/s
v = velocity, m/s
v_c = critical speed below which no impact damage occurs, m/s
v_d = damage or delamination threshold velocity, m/s
v_f = speed of stone after contact with tire, m/s
v_i = impingement velocity, m/s
v_n = absolute component of tire velocity along line connecting mass centers of stone and tire, m/s
v_s = velocity of stone relative to the aircraft, m/s
v_z = vertical component of velocity of tire, m/s
w = integration parameter, m/s
x = horizontal distance between tire–ground and stone–tire contact points, m
y = horizontal displacement along tire axis, m
z = height of tire center above stone center, m
α = stone launch angle above ground in plane of wheel, rad
δ = vertical deflection of tire, m
μ = coefficient of friction or dynamic viscosity, N-s/m^2
μ_g = coefficient of friction between ground and stone
ρ = density, kg/m^3
θ = angle relative to vertical of line intersecting the stone and tire centers, rad
ω = angular velocity, rad/s
ϕ = angle above ground in plane perpendicular to tire motion, rad

Received 10 November 2010; accepted for publication 27 November 2010.

*Research Associate, Department of Aeronautics.
†Reader, The Composites Centre.
‡Senior Scientist, Damage Tolerance, Box 104.

I. Introduction

KNOWLEDGE of runway debris lofting mechanisms is currently very limited, but an improved understanding of these mechanisms provides a means to assess the threat of impact damage. An example of the severity of the impact damage produced by runway debris is shown in Fig. 1, which depicts extensive denting and tearing of the metallic skin of a C-130 Hercules component. The objective of this study is to develop a physically based closed-form analytical model to predict critical runway stone lofting parameters, such as the vertical loft speed, as a function of aircraft and runway conditions. The next section presents an overview of key work on runway debris lofting and background information of the relevant analytical approaches used for modeling impact events and highlights the importance of understanding the fundamental processes underlying stone lofting.

II. Background

A. Previous Lofting Studies

To date, the greatest insight into lofting mechanisms has been provided by high-speed video in experiments with loaded tires overrolling stones [1,2]. These studies are the basis of the design requirements for runway debris for many aircraft. The experiments gave estimates of bounds that could be placed on velocities and directions of lofted stones and enabled potential mechanisms to be confirmed or rejected. They also provided some insight into the

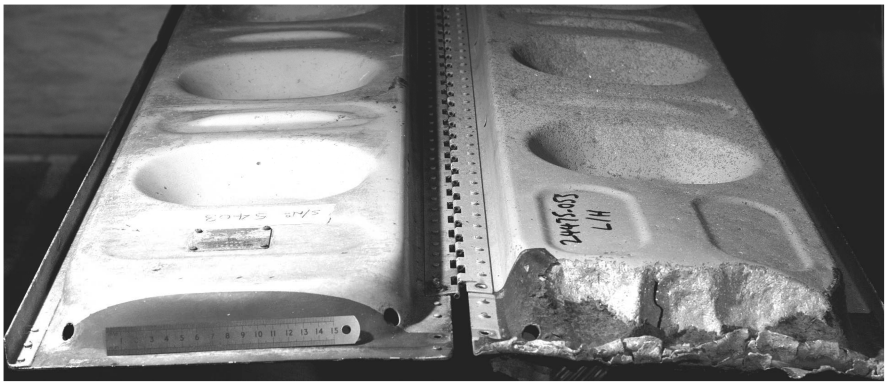

Fig. 1 Photograph of C-130 Hercules main gear undercarriage bay doors. The undamaged trailing edge of the door is shown on the left and the impact damaged leading edge of the component is shown on the right.

influence of parameters such as tire velocities and pressure and runway conditions on lofted-stone trajectories. These previous studies found an exponentially decreasing distribution in the number of stones lofted with regard to increasing loft speed or height. However, there remained controversy as to whether stones were launched from the side or the rear of the tire footprint, which clearly influences the dominant lofting mechanism. Because of the resources required for such experiments, it was difficult to identify clear trends, because the data set of lofted stones was limited and the validity of scaling the results to reflect realistic takeoff and landing speeds was uncertain. Therefore, numerical models have been implemented to gain an insight into the influence of various stone and aircraft parameters on the lofting mechanisms [3–5].

However, for efficient design and sizing of aircraft components, analytical models are more useful. Thus, accompanying the experiments mentioned above, simple analytical models were proposed and suggested that there was the potential for high stone launch speeds to be achieved, despite the major experimental studies only observing low vertical velocities. These models were based on assumed lofting mechanisms, such as a stone being pinched out from beneath a tire tread (pinch lofting) or being struck downward with a rapid glancing blow (hammer lofting). Since the latter mechanism was reported to provide greater consistency with the experimental evidence, the current investigation developed a model based on this mechanism. The equations for determining the initial tire–stone contact speed given in [1] were used as a starting point to develop the analytical model.

B. Ball Impact Models

Numerous analytical studies of dynamic contact between two bodies with friction have been presented in the literature [6–8]. However, the treatment of a body simultaneously in contact with two other bodies having very different material and geometrical properties has been addressed much less extensively. Tire material rubber with an initial tangent modulus of typically 30 MPa [9] may interact with stones and runway surface materials having elastic moduli of approximately 50 and 25 GPa, respectively [9]. Given the range of typical runway stone sizes of up to 30 mm [10] and aircraft takeoff or landing velocities of up to 100 m/s [10], the mechanics of launching sports balls was considered relevant. Many successful predictions of the impact behavior of objects such as golf balls, snooker balls, and cricket balls have been made by using discrete spring-mass-dashpot models [11]. These models have been based on equations of motion constrained by conservation of energy, conservation of momentum, and definitions of normal and tangential coefficients of restitution. Typically, the models have used only a single parameter for the coefficient of friction, corresponding to that occurring after slip has taken place. In cases where considerable deformation occurred, there was no single contact point about which angular momentum would be conserved. This was expected to limit the validity of the analytical solutions for predictions of high-speed events occurring with spin. However, recent studies of deformable ball impacts have shown that the deviations of the rebound angles from rigid-body theory were surprisingly small [12].

C. Significance of Dominant Lofting Mechanisms

To illustrate how an understanding of the governing lofting mechanism can affect structural design decisions, consider the design of a leading-edge component close to a wheel, as shown in Fig. 2a. If tangential lofting were assumed, such that the total speed of the stone v_s relative to the aircraft was equal to that at the outer diameter of the tire (i.e., the aircraft speed V relative to the ground), the maximum normal velocity component upon impact would be $V\cos\alpha$. Take, for example, $\alpha = 60°$ so that $v_n^{\max} = V/2$. In contrast, if the impingement of the aircraft onto the stone is the underlying process, then $v_n^{\max} = V$ and the maximum kinetic energy is four times that predicted by the tangential loft model. A physical interpretation for the cause of this discrepancy is that for the tangential loft model, the stone needed to be pulled forward by the tire to remain in contact with it and follow the upward path of the tread. The forward velocity of the stone reduces the relative horizontal velocity between the stone and the aircraft. For horizontally oriented structures, the effect of incorrectly assuming a tangential loft mechanism would be to underestimate the tangential impact velocity but overestimate the normal

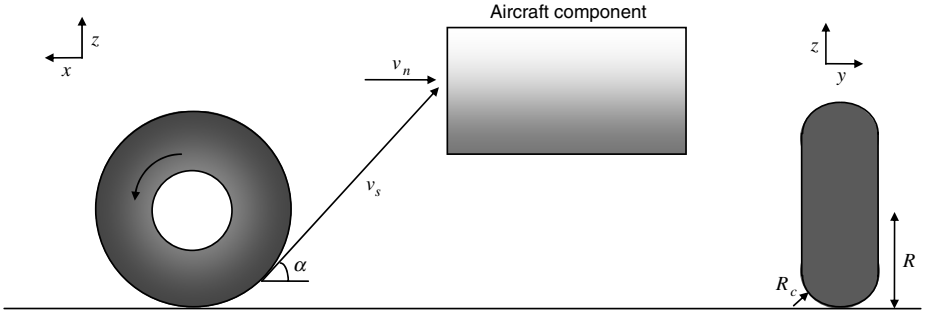

Fig. 2 Illustrations of a) side view of an impact caused by tangential lofting on a component leading edge and b) front view of tire.

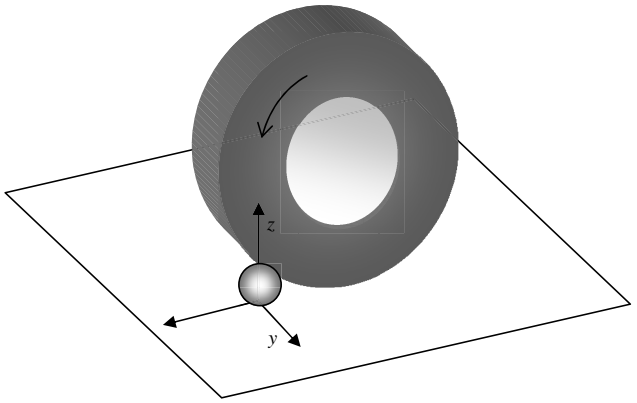

Fig. 3 Definition of coordinate system for analytical modeling of stone lofting.

impact velocity. As a consequence, a design approach based on a simplistic and inaccurate lofting mechanism could result in unnecessarily heavy structures and reduced payload capacity.

III. Initial Tire–Stone Contact Speed

This section concerns analytical modeling of the stone–tire interaction leading to sideward lofting, using a classical mechanics analysis to progressively develop a realistic final model. The first step is to calculate the initial contact speed between the tire and the stone so that the nature of the load applied to the stone could be established. The origin of the coordinate system is at the stone–ground contact point, with the reference axes and planes defined as shown in Fig. 3. The stone is assumed to be spherical and the ground is assumed to be perfectly flat. The ground, the stone, and the tire are assumed to be rigid, and the tire is considered to roll without slip.

For the axes, x is the axis along the direction of aircraft travel, with positive being forward; y is the sideward direction parallel to the tire axis, with positive to the left of the tire; and z is the axis in the vertical direction, with positive taken upward.

For planes, x–y is the ground plane, y–z is the plane that bisects the stone and contains the sideward stone trajectory, and x–z is the plane bisecting the stone and perpendicular to the axis of the tire.

The initial velocity at which the tire surface approaches the stone can be calculated as a function of the geometry and speed of the tire and the geometry of the stone. Two distinct cases were considered:

1) The entire stone was within the tire footprint width.

2) The stone was partially inside the footprint width.

A. Stone at the Center of the Footprint

For complete overrolling of a stone, the vertical and resultant stone–tire contact velocities are shown in Fig. 4. The vertical component of the initial tire–stone contact velocity can be expressed as follows [1] using the derivation shown in the Appendix:

$$v_z = V\sqrt{2h/R - (h/R)^2} \tag{1}$$

The total velocity of initial contact between the tire and the stone can be found by

$$q^2 = x^2 + h^2 \tag{2}$$

$$v = \omega q = \frac{V}{R}\sqrt{2Rh} \tag{3}$$

$$v = V\sqrt{2h/R} \tag{4}$$

The angle relative to the vertical at which initial contact occurs is

$$\theta = \cos^{-1}(v_z/v) \tag{5}$$

$$\theta = \cos^{-1}\sqrt{1 - h/2R} \tag{6}$$

For typical stone and tire parameters, $h = 20$ mm and $R = 0.2$ m, we obtain $\theta = 13°$.

B. Stone at the Edge of the Footprint

The initial contact speeds are slightly different when the stone is at the edge of the tire footprint (Fig. 5) and depends on the angle that the tire shoulder makes with the ground. The tire radius is assumed to be large compared with the stone radius so that the initial contact occurs at a position with an x coordinate close to that of the center of the stone. The derivation given in the Appendix leads to the following expression taken from [1]:

$$v_z = V\sqrt{2h/R - (h/R)^2 + (b/R)^2\tan^2\phi - (2b/R)\tan\phi} \tag{7}$$

C. Tire Deflection

Equation (1) assumes that the tire has no deformation from vehicle loading and rides tangentially to the runway surface. The analysis becomes slightly more complex if it accounts for the finite deflection of the tire surface caused by vehicle loading. This deflection may be expressed in terms of the easily measured footprint length of the tire using Eq. (8) taken from [1] and derived in the Appendix:

$$\delta = R - \sqrt{R^2 - L^2/4} \tag{8}$$

If the assumption is made that the tire surface clear of the runway is undistorted by runway contact, the tire deflection may simply be added to the height h of the contact point on the stone when calculating the speed of tire–stone contact, Fig. 6. Thus, Eqs. (7) and (8) provide a simple, complete, and relatively accurate computation for the downward-directed velocity of a tire tread as it contacts a

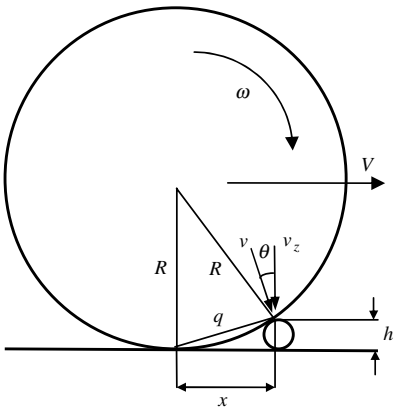

Fig. 4 Kinematics of rolling over a stone at the center of the tire footprint.

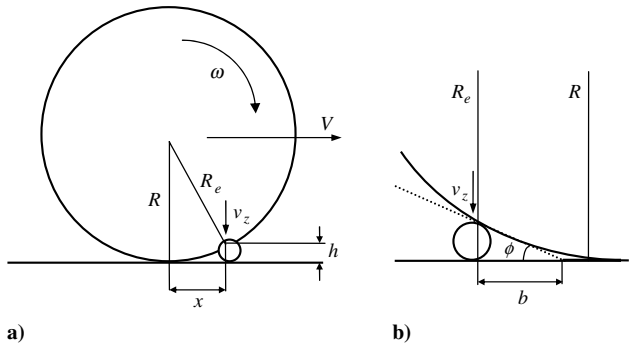

Fig. 5 Illustrations of a) right side view of tire–stone contact at the edge of the tire footprint and b) rearward view of contact between tire and stone.

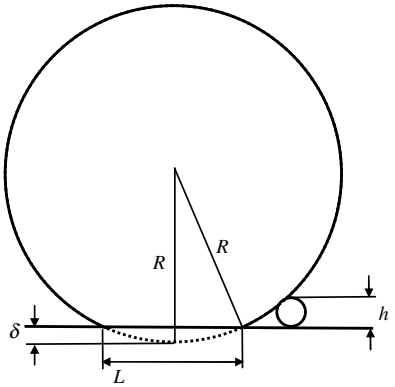

Fig. 6 Vertical deflection of tire due to vehicle load.

stone surface as a function of stone height, tire geometry, and aircraft forward velocity [1].

For an aircraft tire, the vertical deflection is also a function of the aircraft speed, due to greater lift at higher speeds. An initial approximation would be to assume that the deflection varies with the square of the tire speed, taking a maximum value when the tire is stationary and having zero deflection when the aircraft reaches the takeoff or landing speed:

$$\delta = \delta_0[1 - (V/V_T)^2] \tag{9}$$

IV. Runway Stone Loft Model

A starting point for developing a lofting model governed by a hammer mechanism involved simplifying the problem by treating the tire–stone and stone–ground interactions as independent events. Figure 7a details the contact between the tire, stone, and ground.

This model relies on the assumption that although the stone receives forces from the two surfaces simultaneously, because the surfaces are not identical, the stone will leave one surface before the other. The simplified two-dimensional loft model developed here treats the stone, ground, and tire as rigid and later introduces friction into the interactions.

A. Frictionless Tire–Stone and Stone–Ground Interactions

Consider the motion of a tire rolling over a stone as a rigid-body collision. A mass m_t is assigned to the section of tire striking the stone to enable calculation of the momentum that may be transferred. Later, the tire mass is assumed to be much greater than the stone mass. Immediately before impact (Fig. 7a), the absolute component of the tire velocity v_n along the line connecting the centers of mass of the stone and the tire is

$$v_n = v_z \cos\theta = \frac{z}{R_c + r} v_z \tag{10}$$

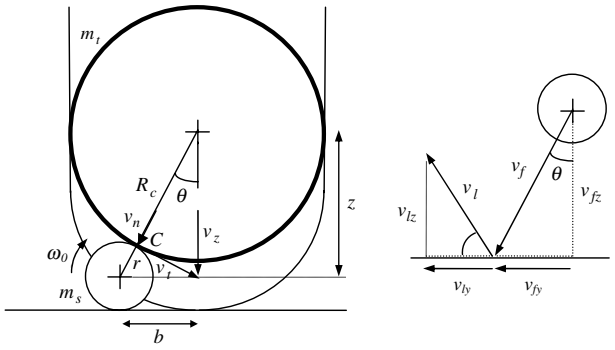

a) b)

Fig. 7 Illustrations of a) vertical cross section of interaction between tire, stone, and ground and b) stone velocities after impact from tire and rebound from ground.

where the vertical velocity component of the section of tire descending upon the stone can be approximated using Eq. (1). In the special case of frictionless interactions, $v_t = \omega_0 = 0$. By combining the definition of the coefficient of restitution with conservation of momentum, the final speed of the stone after the collision with the tire is [6]

$$v_f = \frac{(1 + e_t) m_t v_n}{m_s + m_t} \tag{11}$$

A diagram detailing the kinematics of the impact between the stone and the ground is shown in Fig. 7b. If the ground is smooth, the velocity component of the stone parallel to the ground is unaffected. The vertical component of the stone loft velocity is given by

$$v_{lz} = e_g v_f \cos\theta \tag{12}$$

Combination of Eqs. (10) and (11) and use of the geometrical relations in Fig. 7b then yields

$$\begin{aligned} &= e_g \frac{(1 + e_t)}{m_s/m_t + 1} \frac{(R_c + r)^2 - b^2}{(R_c + r)^2} v_z \\ &= \frac{e_g(1 + e_t)}{m_s/m_t + 1} \left[1 - \left(\frac{b}{R_c + r}\right)^2\right] v_z \end{aligned} \tag{13}$$

If the mass of the stone is much smaller than the mass of the tire, i.e., $m_s \ll m_t$, then

$$v_{lz} = e_g(1 + e_t)\left[1 - \left(\frac{b}{R_c + r}\right)^2\right] v_z \tag{14}$$

The maximum value of v_{lz} would occur when $e_g = e_t = 1$, $b = 0 = > v_{lz} \approx 2v_z$. The maximum value of v_z within the range of expected stone and tire diameters is $v_z \approx 0.5V$. Hence, the maximum vertical loft velocity is approximately the speed of the aircraft. However, this scenario would not be possible, since the stone would strike the tire after it rebounded from the ground. There would be repeated rebounds until the tire moved out of the path of the stone. If the offset distance is such that $b > 0$, the stone may still clip the lower surface of the tire after bouncing off the ground. The vertical speed of the stone would be reduced by this rebound, but its maximum speed may still be approximated by the expression above. The actual loft speed would depend on the number of rebounds between the stone, the ground, and the tire.

B. Tire–Stone and Stone–Ground Friction

When friction is introduced between the tire and stone, the tangential component of the impact velocity can cause the stone to spin, as shown in Fig. 7a. Assuming that there is no slip at contact point C, the stone is given an angular velocity:

$$\omega_0 = \frac{v_t}{r} = \frac{v_z \sin\theta}{r} = \frac{y v_z}{r(R_c + r)} \tag{15}$$

For a spherical stone, the ground friction will not affect the vertical loft velocity, but will influence the spin and horizontal velocity. Applying general equations of motion for impacts with friction [6] to the current loft model gives

$$v_{ly} = v_{fy} - \mu_g(1 + e_g) v_{fz} \tag{16}$$

$$\omega_l = \omega_0 - \mu_g \frac{r}{l_s^2}(1 + e_g) v_{fz} \tag{17}$$

This leads to the following translational and angular velocities for the lofted stone:

$$v_{ly} = \frac{(1 + e_t)}{m_s/m_t + 1} \left\{ \frac{bz}{(R_c + r)^2} - \mu_g(1 + e_g)\left[1 - \left(\frac{b}{R_c + r}\right)^2\right] \right\} v_z \tag{18}$$

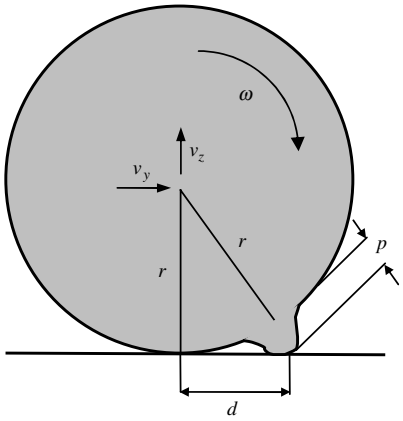

Fig. 8 Kinematics of asperity lofting of a stone radius *r*.

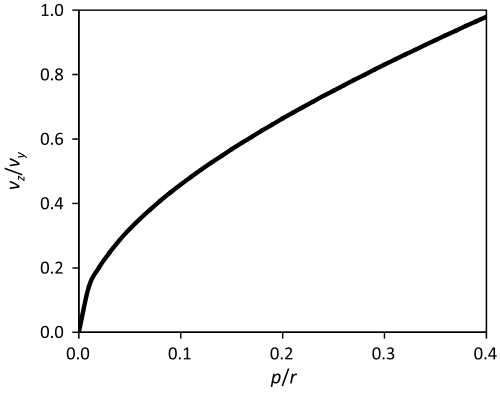

Fig. 9 Variation of vertical loft velocity obtained using Eq. (23) with the asperity height.

$$\omega_l = \left\{ \frac{b}{r(R_c + r)} - \frac{r}{l_s^2} \frac{\mu_g (1 + e_g)(1 + e_t)}{m_s/m_t + 1} \left[1 - \left(\frac{b}{R_c + r} \right)^2 \right] \right\} v_z \tag{19}$$

$$v_{lz} = \frac{e_g (1 + e_t)}{m_s/m_t + 1} \left[1 - \left(\frac{b}{R_c + r} \right)^2 \right] v_z \tag{20}$$

C. Asperity Lofting

This section briefly considers the potential lofting of a rigid stone of irregular geometry, in which the irregularity is idealized as a single protrusion on the surface of the stone with a height p above the average radius of the stone (Fig. 8). An interaction between the protrusion and the ground can lead to the stone attaining a vertical velocity in two ways [1]. The protrusion can dig into the ground causing a horizontally moving stone to be levered upward by rotating about the asperity tip. Alternatively, a spinning stone, whether initially translating or not, can be propelled with a vertical velocity as the protrusion strikes the ground. The following equations can be used to quantify the ratio of the vertical loft velocity to the initial horizontal or tangential surface velocity of the stone:

$$d = \sqrt{(r + p)^2 - r^2} \tag{21}$$

$$v_z = d\omega = dv_y/r \tag{22}$$

$$v_z/v_y = (p/r)\sqrt{2r/p + 1} \tag{23}$$

Plots of the vertical velocity and the corresponding loft angles as functions of the asperity height are shown in Fig. 9. Stones of realistic asperity heights were therefore expected to obtain loft angles up to 45° via this asperity lofting mechanism [1] if the ground surface is flat.

D. Analytical Model Parameters

The results for the rigid-body model were calculated using Eq. (20) and implemented in MATLAB 6.5. The default parameters used in this model were $r = 10$ mm, $R = 0.2$ m, $V = 70$ m/s, $l = 30\%$, $R_c = 1$ mm, $\mu_g = 0.6$, $\mu_t = 0.65$, $e_g = 0.7$, $e_t = 0.6$, $\rho_s = 2700$ kg/m^3, and $m_t = 65$ kg. A very small tire cross-sectional radius R_c was chosen to simulate the impact by a sharp cornered tire for later comparison with modified drop-weight experiments. Values for the coefficient of restitution for materials relevant to runway debris lofting were estimated based on data in the literature for objects of similar geometrical and material properties [13]. These values were functions of the relative impact velocity v_i, and empirical relationships found by curve fits to experimental data are shown in Table 1. It should be noted that experimental values for the coefficient of restitution exhibit considerable scatter making it difficult to obtain a single reliable value. For instance, when $v_i = 35$ m/s, the coefficients of restitution for a 22 mm steel ball and a 16 mm glass ball against 56 mm rubber were calculated to be 0.61 and 0.50, respectively. Hence, the approximation of $e_t = 0.6$ was chosen because the mean value of 0.56 was rounded to the nearest decimal place to reflect the low accuracy of the estimate. Note that actual tire rubber material would be thinner than that used to obtain the coefficient of restitution values in Table 1. Assuming the stone strikes the ground at the same relative impact velocity, and assuming that the ground behaves in a similar way to the slate surface, the values of e for a 22 mm steel ball and a 16 mm glass ball against a slate surface were 0.65 and 0.75, respectively. Hence, the mean value of $e_g = 0.7$ was chosen. In the rigid-body model, the tire cross-sectional radius, the stone density, the mass of the tire and the stone–ground coefficients of friction had a negligible effect on the vertical loft velocity within the range of values of interest.

Stone diameters were varied from 10 mm to 30 mm to model stones considered large enough to cause damage but small enough to have a significant likelihood of being encountered [10]. The baseline value was the median of this range and was chosen to simplify specification of the overlap. Tire diameters varied from 0.4 m to 1.4 m to consider the whole range of nose and main wheel tire sizes that may be used [14]. The baseline value was 0.4 m, because this was a typical value for a nose wheel of a fast military aircraft, which was expected to be responsible for the most critical impact scenarios. The tire speed was varied from 0 m/s to 100 m/s to account for the full range of takeoff and landing velocities of military and civil aircraft [14]. The baseline value of 70 m/s was chosen, since this was the mean takeoff velocity of military aircraft [10], which were most susceptible to runway stone damage.

The overlap was varied from 0 to 50% of the stone diameter to consider all instances in which the center of the stone was not within

Table 1 Coefficient of restitution for various impact configurations [13]

Rebounding object	Target surface	Empirical relationship	e for $v_i = 35$ m/s
22 mm steel ball	56 mm rubber	$e = 0.6809 v_i^{-0.0293}$	0.61
22 mm steel ball	31 mm slate	$e = 0.7498 v_i^{-0.0405}$	0.65
16 mm glass ball	56 mm rubber	$e = 0.6696 v_i^{-0.0842}$	0.50
16 mm glass ball	31 mm slate	$e = 0.8526 v_i^{-0.0343}$	0.75

the tire footprint and was therefore expected to produce sideward lofting. Overlaps greater than 50% were considered to result in tangential lofting for which the tire speed could be used as a conservative estimate for the impact speed. Since any overlap was equally likely, the default overlap used for all of the analytical models was chosen to be 30%, because this was roughly midway between the two extremes and was rounded to the nearest 10% for simplicity.

The coefficient of restitution values used in the rigid-body impact analysis would clearly influence the results of this model. From Eq. (23), the vertical loft speed was directly proportional to the stone–ground coefficient of restitution and a linear function of the tire–stone coefficient of restitution. The baseline stone density was 2700 kg/m^3, since this was the mean density of stone material collected from runways in a previous study [10] and also the density of aluminum, the material used for some aircraft parts and fasteners. To restrict the scope of the parametric study, the influence of this variable was not studied in detail here. This was justified by the low variance in stone densities over the range of stone types observed on runways [10].

The mass of the wheel assembly was a parameter specified in the rigid-body impact model, and its baseline value was 65 kg, which was the mass of a typical aircraft wheel [15]. The influence of this parameter was also not the subject of a detailed study. Since the tire mass was three orders of magnitude greater than the stone mass, the effect of realistic variations in tire mass was expected to be negligible. The tire cross-sectional radius took a baseline value of 1 mm, suggesting that an unrealistically sharp tire was modeled. However, the tire cross-sectional radius had negligible influence on the results, because the rigid-tire assumption implied the stone–tire contact was made at an infinitesimally small point. Therefore, the effect of different tire cross-sectional radii could be captured in varying the overlap.

V. Results

In this section, the results of the analytical lofting model are presented in terms of the vertical stone loft velocity, which was considered to be the most critical velocity component for primary aircraft structures.

A. Parametric Studies

The vertical loft speed was directly proportional to the overlap for overlaps up to 20% (Fig. 10) and approached a maximum at 50% overlap. At any given overlap, larger stones were lofted at higher speeds (Fig. 11). For instance, with an overlap of 30%, doubling the stone diameter from 10 to 20 mm increased the vertical loft speed by 42% from 19 to 27 m/s. For a given stone size, increasing the overlap also led to greater vertical loft speeds, because the direction of the initial relative velocity was closer to the vertical. The vertical loft speed was directly proportional to the tire speed (Fig. 12) and was approximately 40% of the tire speed using the default model parameters. Larger tires resulted in lower vertical loft speeds, as shown in Fig. 13. For instance, a 1-m-diam Hercules nose wheel could produce vertical loft speeds of 18 m/s, whereas the corresponding speed for the 1.4-m-diam main wheel was 15 m/s. In terms of the sensitivity of the vertical loft velocity to the stone parameters studied, the stone position relative to tire was the most important parameter for all the models. Therefore, the plot of vertical loft speed against overlap (Fig. 10) was useful for comparison with experimental and numerical results.

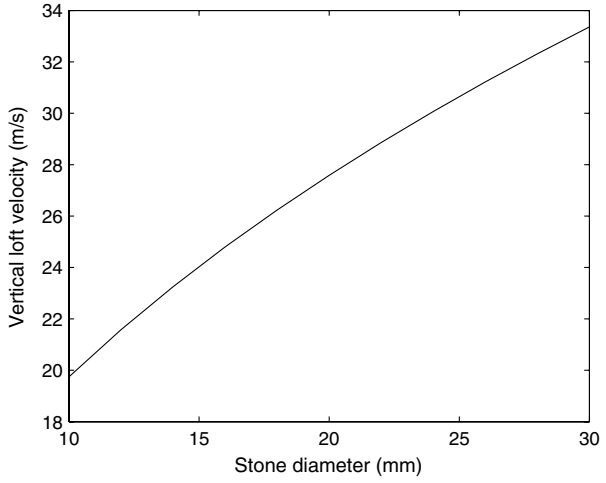

Fig. 11 Influence of stone size obtained using Eq. (20).

B. Comparison with Experimental Lofting Studies and Predictions

For aluminum spheres of 14 mm diameter, a comparison was made between the analytical rigid lofting model and modified drop-weight impact experiments [3], as shown in Fig. 14. The modified drop-weight experiments involved a steel impactor covered with reinforced rubber descending upon an aluminum sphere positioned on a steel base. The trajectory of the sphere after impact was recorded using high-speed video to obtain the loft velocities and angles. These experiments were also simulated using finite element (FE) software (LS-DYNA) to provide validation of the lofting mechanisms predicted by the FE models.

The majority of the experimental data points were captured within the envelope defined by the analytical loft model. The vertical loft velocity of 11 mm spheres against overlap was also plotted for the analytical solution, drop-weight numerical simulation and the experimental results (Fig. 15). The analytical solution produced an envelope that captured all but two of the data points, but was highly conservative at overlaps greater than 35%. The simulated velocities

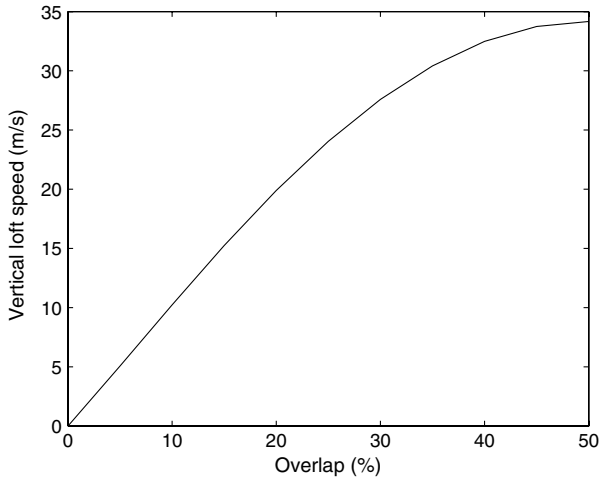

Fig. 10 Influence of overlap obtained using Eq. (20).

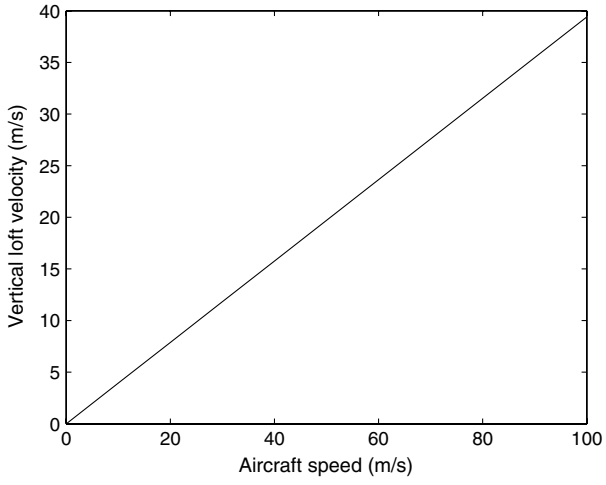

Fig. 12 Influence of tire speed obtained using Eq. (20).

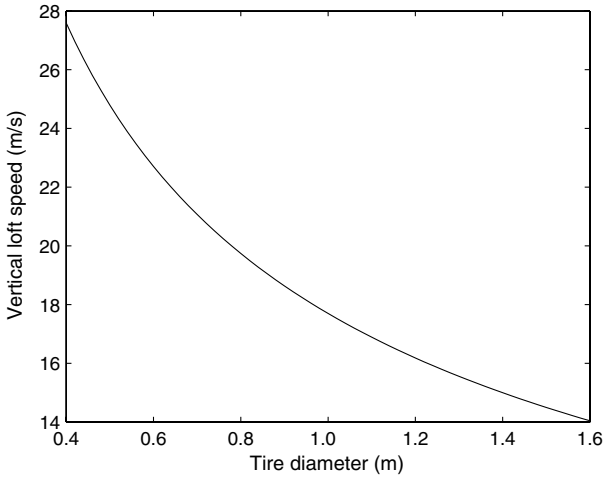

Fig. 13 Influence of tire diameter obtained using Eq. (20).

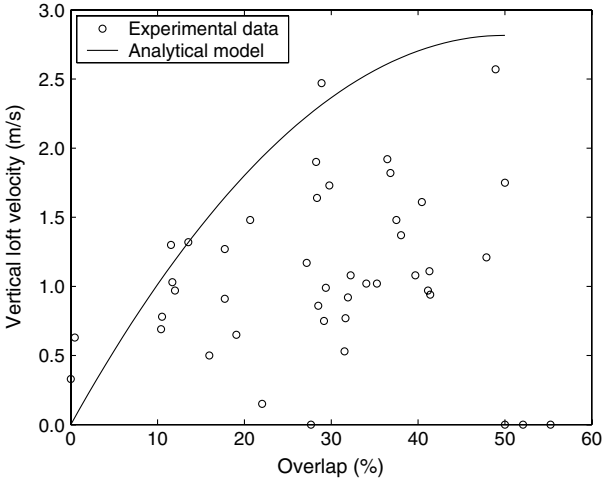

Fig. 14 Comparison between drop-weight experiments for 14 mm spheres impacted at 4.4 m/s with $e_g = 0.4$ and analytical model results obtained using Eq. (20).

gave a reasonable upper-bound envelope to the scattered experimental data for values of overlap up to one-third of the stone diameter. For larger values of overlap, the numerical predictions were not as conservative; an overlap of one-half of the sphere diameter resulted in several instances where the experimental loft velocities exceeded the numerical predictions. Neither the analytical nor the numerical models were able to accurately predict the experimental loft speeds at overlaps between 35 and 50%, although the analytical model was considered more suitable for conservative design predictions. In the numerical simulations, at overlaps approaching half the stone diameter, the rubber simply enveloped the stone and prevented the stone from escaping. However, in the experiments, at high values of overlap, local rupture of the rubber could occur, allowing the stone to be projected at velocities similar to those at lower overlaps. This was a phenomenon that the simulations could not capture, since the material model used for the rubber did not include failure.

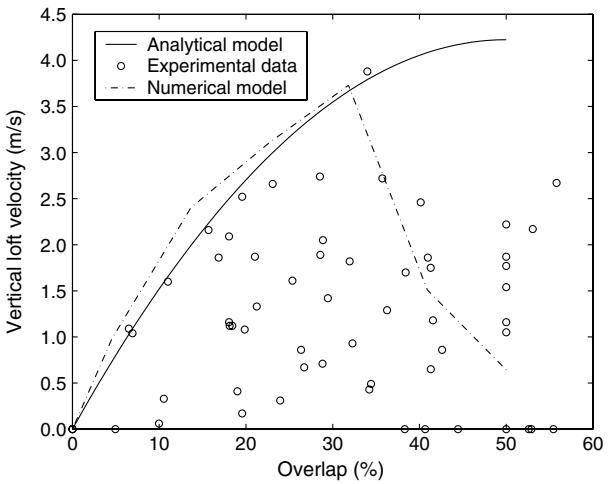

Fig. 15 Vertical loft velocity against overlap for 11 mm spheres impacted at 4.4 m/s with $e_g = 0.4$. The analytical solution was obtained using Eq. (20).

VI. Influence of Air Resistance and Gravity

To consider the importance of including the drag and gravity in an analysis of lofted-stone trajectories, the current section includes calculations of the associated reductions in impact velocity under typical lofting conditions. The first two subsections consider the influence of air resistance and gravity separately, and the final subsection summarizes the significance of both when evaluating the impact threat from stones.

A. Influence of Air Resistance

Assuming a quadratic relationship [16] between the drag force and the stone velocity, the deceleration of a stone can be expressed as

$$\frac{\mathrm{d}v}{\mathrm{d}t} = -\frac{C_D \rho_a A}{2m} v^2 \tag{24}$$

$$-v^{-2}\frac{\mathrm{d}v}{\mathrm{d}t} = K \tag{25}$$

where

$$K = \frac{C_D \rho_a A}{2m} = \frac{C_D \rho_a \pi r^2}{2\rho_s (4/3)\pi r^3} = \frac{3C_D \rho_a}{8\rho_s r} \tag{26}$$

Let

$$w = v^{-1} \tag{27}$$

$$\frac{\mathrm{d}w}{\mathrm{d}t} = K \tag{28}$$

$$w = Kt + C \tag{29}$$

$$v = \frac{1}{Kt + C} \tag{30}$$

When $t = 0$, then $v = v_0$. Therefore, $C = 1/v_0$, and the speed of the stone as a function of time is

$$\frac{v}{v_0} = \frac{1}{Kv_0 t + 1} \tag{31}$$

To find the speed of the stone as a function of the distance traveled, Eq. (32) is solved with the initial condition $s(t = 0) = 0$, which yields Eq. (33):

$$\frac{\mathrm{d}s}{\mathrm{d}t} = \frac{1}{Kt + C} \tag{32}$$

$$s = \frac{1}{K}\ell_n\left(\frac{Kt}{C} + 1\right) \tag{33}$$

$$e^{Ks} = Kt/C + 1 \tag{34}$$

$$t = \frac{C}{K}(e^{Ks} - 1) \tag{35}$$

$$v = \frac{1}{Kt + C} \tag{36}$$

$$v = \frac{1}{C(e^{Ks} - 1) + C} \tag{37}$$

$$v = 1/Ce^{Ks} \tag{38}$$

$$v/v_0 = e^{-Ks} \tag{39}$$

$$\frac{v}{v_0} = \exp\left(-\frac{3C_D\rho_a s}{8\rho_s r}\right) \tag{40}$$

Therefore, the fractional reduction in speed is given by

$$\frac{v_0 - v}{v_0} = 1 - \frac{v}{v_0} = 1 - \exp\left(-\frac{3C_D\rho_a s}{8\rho_s r}\right) \tag{41}$$

The maximum reduction in speed occurs when this ratio takes the highest value. A low-density stone, a large distance traveled, and a small stone radius all result in maximum aerodynamic drag. Using typical values [9,10,17] ($C_D = 0.5$, $\rho_a = 1.22$ kg/m^3, $\rho_s =$ 2680 kg/m^3, $s = 1$ m, and $r = 10$ mm), the reduction in speed of the stone is 0.85%. Therefore, in the short distance required for the stone to travel from the ground up to a height such that it could impinge on an aircraft component, the effect of air resistance is small enough to be neglected. For a smaller stone of $r = 5$ mm, the speed reduction of 1.7% may justify an analysis including air resistance, although it is likely that such small stones would result in negligible impact damage.

B. Influence of Gravity

Clearly, it is necessary to consider the effect of gravity for low vertical loft speeds, but for higher speeds the effect of gravity becomes less important. The reduction in speed depends on the height of travel q as well as the initial loft speed v. The minimum travel height of interest is the lowest vulnerable point on the aircraft. The maximum height of interest is the highest vulnerable point or the maximum height that the stone can reach, whichever is lower. By equating the change in the vertical translational kinetic energy with the change in the gravitational potential energy, the change in speed due to gravity is

$$\Delta v = v_0 - v = v_0 - \sqrt{v_0^2 - 2gq} \tag{42}$$

Suppose that a vertical impact velocity of 30 m/s is needed to initiate damage in a horizontal fuselage panel 1 m above ground. The reduction in speed due to gravity is 0.33 m/s, which is 1.1% of the initial speed. This small gravitational effect implies that for impact speeds liable to cause damage to horizontal structures, a conservative approach would be to simply take the impact speed as the initial loft speed.

VII. Discussion

A. Parametric Studies

The rigid-tire model predicted that for a given overlap, larger stones were able to achieve greater loft speeds. This trend was essentially because the contact with the tire was made at a greater height, and therefore the vertical velocity component of the tire upon initial contact with the stone was greater. The predicted relationship between the vertical loft speed and the aircraft speed was one of direct proportionality, because the tire speed determined the initial tire–stone contact speed. On the other hand, the reduction of loft speeds with increasing tire diameter was due to a decreasing initial contact speed with the stone, as was evident in Eq. (1). The results of the analytical models suggested that the parameters that needed to be modeled correctly to accurately predict stone lofting were geometrical properties of the tire local to the stone–tire contact zone.

One of the main limitations of the rigid-body model arose from the assumption of idealized geometry for the stone and tire, which led to simplified equations for collinear impacts being applied. In reality, for the impact between the tire and the stone, the impact is not collinear, because the center of mass of the tire is not on a common normal line passing through the point of contact. Furthermore, the irregular shape of most stones also results in the impact deviating from the collinear case. Realistic deviations from the idealized case would not only impose a significant scatter on the loft speeds and angular velocities, but to also introduce further velocity components not considered in the current analysis. The complexity of such an analysis highlighted the advantages of numerical methods in further model development and stochastic approaches to quantify the uncertainty associated with the impact threat from runway stones.

B. Comparison of Analytical, Numerical, and Experimental Lofting Studies

Various sources of energy dissipation that were not accounted for in the analytical model resulted in many of the experimental lofts occurring at much lower vertical velocities than those predicted. Lofts at overlaps greater than 30%, which could exceed the simulated values, were considered to be a result of higher loft angles than expected. This discrepancy may have been related to modeling the ground surface as flat, while the experimental set up used rough sandpaper to achieve realistic friction coefficients. As found in previous FE simulations [5], at the same overlap of 30%, increasing the ground–stone friction had hardly any effect on the vertical loft velocity, but decreased the total velocity. Therefore, the loft angle increased with increasing ground–stone friction. At the higher values of overlap, the asperities in the ground surface resulted in a greater interaction of the stone against the ground, compared with the model, and hence higher vertical loft velocities. The model predictions were expected to be less accurate for greater overlaps, when large local strains could be achieved and the material properties became more important. Therefore, greater attention should be paid to modeling the behavior of the tire material in this regime, where the tread deformation may be large enough to cause local rupture of the rubber.

C. Asperity Lofting

Optimal structural design should consider the dependence of the impact threat on the location of the structure relative to the wheels. Away from the wheels, there has been no experimentally observed mechanism that could produce impacts with large vertical velocity components, except for asperity lofting. Because of the random geometry and spacing of the asperities, it could be inferred that relative to the ground, any asperity loft direction was theoretically possible, including those forward of the lofting wheel. A small degree of forward lofting relative to the ground has been observed in tests carried out at the University of Dayton Research Institute [1]. However, the analytical modeling and drop-weight experiments [3] showed that the maximum speed produced by this mechanism was approximately half the aircraft speed. Hence, the resulting impact location would be well behind the wheel, as observed on C-130 Hercules aircraft [4].

Under conditions in which asperity lofting may be prevalent, significant normal impact speeds may be attained if the rebound directs the majority of the momentum of the stone in an upward direction. Based on this lofting mechanism, a conservative design would be to consider a normal velocity threshold of half the takeoff velocity over the entire underbelly of the aircraft rearward of the nose wheel. A first attempt at quantifying the probabilistic threat presented by such a scenario would be to assume that there is an equal likelihood of any direction being taken after striking an asperity. Thus, the probability that the vertical velocity component exceeds a

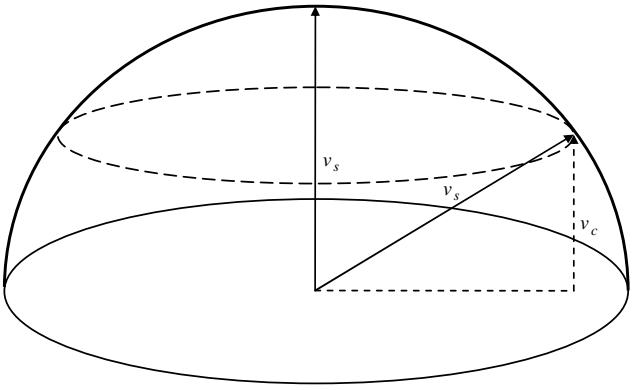

Fig. 16 Possible asperity loft directions with vertical speeds $>v_c$.

critical value v_c can be calculated by considering the ratio of surface areas of a spherical cap within a hemisphere representing all possible rebound angles in three dimensions (Fig. 16). The radius of the hemisphere is the initial stone launch speed v_s and the surface areas of the cap and the hemisphere can be expressed using standard geometrical formulas to give the following expression:

$$P(v_z > v_c) = \frac{2\pi v_s(v_s - v_c)}{2\pi v_s^2} = 1 - \frac{v_c}{v_s} \tag{43}$$

This analysis also assumes the worst-case scenario that the speed of the stone after rebound is equal to that before rebound. For a very glancing impact of the stone against the asperity, the stone speed may not be affected much and so this assumption is valid. However, when large changes of direction occur, the stone speed would be significantly reduced and would be dependent on the coefficient of restitution between the stone and the asperity. Graphically, the effect of this would be to skew the shape of the hemisphere, so that it would appear more elongated toward the direction of the initial stone launch. Further refinements to the stone trajectories may be introduced by including an analysis of the influence of gravity and drag as presented in Sec. VI.

The critical vertical velocity v_c can be chosen to be one of two relevant velocities. The first, v_i, is the vertical speed required for impingement with the aircraft such that a glancing impact may occur with horizontal surfaces or normal impact may occur with vertical surfaces: e.g., leading-edge structures. Alternatively, v_d may be used in place of v_c to calculate the probability of an impact with a vertical velocity exceeding a damage threshold, or delamination threshold in the case of a composite structure [18]. For instance, suppose the aircraft takeoff speed is 70 m/s and the maximum stone launch speed is 35 m/s. If the delamination threshold velocity is 30 m/s, then the probability of the vertical velocity of a stone exceeding this value, due to asperity lofting is $1 - v_d/v_s = 1 - 30/35 = 1/7$. Of course, a true estimate of the threat would need to include the probability of a sideward launched stone striking an asperity in the first place. This would depend on the properties of the runway surface used such as the roughness and the presence of loose material. Considering the more realistic case of a stone–ground coefficient of restitution less than unity implies that the stone does not need to rebound purely vertically to achieve a maximum vertical velocity (Fig. 17). Neglecting friction to simplify the analysis, leads to the following expression for the maximum vertical stone velocity:

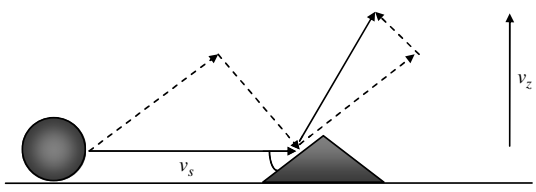

Fig. 17 Asperity lofting of a horizontally launched stone.

$$v_z = v_s \cos\phi \sin\phi + e v_s \sin\phi \cos\phi \tag{44}$$

$$= v_s(1 + e) \sin\phi \cos\phi \tag{45}$$

$$\frac{\mathrm{d}v_z}{\mathrm{d}\phi} = v_s(1 + e) \cos 2\phi = 0 \quad \text{when } \phi = 45^\circ \tag{46}$$

$$v_z^{\max} = v_s(1 + e)/2 \tag{47}$$

If the coefficient of restitution for impacts of objects and materials relevant to debris lofting is approximately $e = 0.6$ [13], then $v_z^{\max} = 0.8v_s$. Therefore, if $v_s = 35$ m/s, $v_z^{\max} = 28$ m/s. This would imply that actually a damage threshold of $v_d = 30$ m/s would not be reached, even if the stone were to travel directly upward after interacting with the asperity. Hence, a design velocity threshold of $V(1 + e)/4$ should be used to ensure that no damage can be produced by asperity lofting. Introducing friction would change the rebound angle required to achieve $v_z^{\max}$, but would also decrease $v_z^{\max}$, so the above design threshold would still be conservative. Another factor not taken into account in this analysis was stone spin. Since this was likely to reduce the translational velocity and only contribute to surface damage, the above analysis is still valid where internal damage is the critical concern.

D. Conditions Affecting Stone Trajectory

For leading-edge damage, the aircraft needs to be traveling at a speed $V > V_c$ and the stone must be lofted with a vertical speed $v_z > \sqrt{(2gq)}$ to reach the aircraft. In addition, the vertical loft speed must be great enough to strike the aircraft before the aircraft passes over the stone. In this scenario, gravity is significant, but air resistance is insignificant. For damage induced by high loft speeds, the aircraft can travel at any speed greater than the speed required to cause lofting of stones such that $v_z > v_c$. In this case, air resistance can be significant for small stones only, but gravity is insignificant. Since both effects act to reduce the impact velocity, an analysis that neglects gravity and air resistance would result in conservative structural design. It is anticipated that these effects are likely to be less important than the effects of air flow around the engines or strong winds, which may be highly unpredictable and may result in more a severe impact speed or a greater probability of impact.

VIII. Conclusions

In summary, the analytical models propose a physical interpretation of runway stone lofting processes observed in previous numerical simulations and experiments. These processes are very sensitive to a large range of parameters, particularly those related to the geometry and mechanical properties of the tire tread local to the stone–tire contact zone. The model predicted an increase in the vertical loft velocity of the stone with increasing stone–tire overlap, stone size, and aircraft speed and with decreasing tire diameter. Under typical operating conditions, the range travel of a stone that impacts an aircraft fuselage would be such that reductions in the impact velocity due to air resistance and gravity would be small in comparison with the impact speed required to initiate damage. Thus, it was concluded that the initial stone launch speeds provided reasonably accurate and conservative predictions of the final impact speeds in the absence of any other significant aerodynamic effects.

However, due to the complexity of stone lofting under realistic conditions, the analytical model was unable to capture important details such as nonlinear material behavior and strain rate effects for which more sophisticated finite element analysis methods may be suitable. Additional validation of these analytical models and any subsequent numerical models are necessary if they are to be used as reliable tools for predicting the threat of runway debris impact damage. Asperity lofting due to the irregular surfaces of the stone and the ground presents a possible mechanism for stones to acquire trajectories that are essentially randomly distributed around the initial launch location. These trajectories lead to a simple quantitative

estimate of the probability of the stone loft velocity exceeding a critical speed sufficient to cause damage to an aircraft structure. The design threshold against impacts occurring due to this mechanism is governed primarily by the maximum takeoff or landing velocity of the aircraft.

Appendix: Initial Tire–Stone Contact Equations

For a stone at the center of the footprint,

$$x^2 = R^2 - (R-h)^2 \tag{A1}$$

$$v_z = \omega x = \frac{V}{R}\sqrt{2Rh - h^2} \tag{A2}$$

$$v_z = V\sqrt{2h/R - (h/R)^2} \tag{A3}$$

For a stone at the edge of the footprint,

$$R_e = R - b\tan\phi \tag{A4}$$

$$x^2 = R_e^2 - (R-h)^2 \tag{A5}$$

$$v_z = \omega x = \frac{V}{R}\sqrt{2Rh - h^2 + b^2\tan^2\phi - 2Rb\tan\phi} \tag{A6}$$

$$v_z = V\sqrt{2h/R - (h/R)^2 + (b/R)^2\tan^2\phi - (2b/R)\tan\phi} \tag{A7}$$

For tire deflection,

$$(R-\delta)^2 = R^2 - (L/2)^2 \tag{A8}$$

$$\delta^2 - 2R\delta + L^2/4 = 0 \tag{A9}$$

$$\delta = R - \sqrt{R^2 - L^2/4} \tag{A10}$$

Acknowledgments

The authors kindly acknowledge the support of Engineering and Physical Sciences Research Council and Defence Science and Technology Laboratory, U.K. Ministry of Defence, for funding this research.

References

[1] Bless, S. J., Cross, L., Piekutowski, A. J., and Swift, H. F., "FOD (Foreign Object Damage) Generation by Aircraft Tires," Defense Technical Information Center, Rept. ESL-TR-82-47, Washington, D.C., 1983.

[2] Beatty, D. N., Readdy, F., Gearhart, J. J., and Duchatellier, R., "The Study of Foreign Object Damage Caused by Aircraft Operations on Unconventional and Bomb-Damaged Airfield Surfaces," BDM Corp., Rept. ADA117587, Mclean, VA, 1981.

[3] Nguyen, S. N., Greenhalgh, E. S., Olsson, R., Iannucci, L., and Curtis, P. T., "Modeling the Lofting of Runway Debris by Aircraft Tires," *Journal of Aircraft*, Vol. 45, No. 5, 2008, pp. 1701–1714. doi:10.2514/1.35564

[4] Nguyen, S. N., Greenhalgh, E. S., Olsson, R., Iannucci, L., and Curtis, P. T., "Improved Models for Runway Debris Lofting Simulations," *The Aeronautical Journal*, Vol. 113, No. 1148, 2009, pp. 669–681.

[5] Nguyen, S. N., Greenhalgh, E. S., Olsson, R., Iannucci, L., and Curtis, P. T., "Parametric Analysis of Runway Stone Lofting Mechanisms," *International Journal of Impact Engineering*, Vol. 37, No. 5, 2009, pp. 502–514. doi:10.1016/j.ijimpeng.2009.11.006

[6] Stronge, W. J., *Impact Mechanics*, 1st ed., Vol. 1, Cambridge Univ. Press, Cambridge, England, U.K., 2000, pp. 35–62.

[7] Arakawa, K., Mada, T., Komatsu, H., Shimizu, T., Satou, M., Takehara, K., and Etoh, G., "Dynamic Contact Behavior of a Golf Ball During Oblique Impact: Effect of friction Between the Ball and Target," *Experimental Mechanics*, Vol. 47, No. 2, 2007, pp. 277–282. doi:10.1007/s11340-006-9018-4

[8] Brach, R. M., *Mechanical Impact Dynamics: Rigid Body Collisions*, Wiley, New York, 1991.

[9] Cambridge Engineering Selector, Software Package, Ver. 2009, Granta Design, Ltd., Cambridge, England, U.K., 2009.

[10] Greenhalgh, E. S., Chicester, G. A. F., Mew, A., Slade, M., and Bowen, R., "Characterisation of the Realistic Impact Threat from Runway Debris," *The Aeronautical Journal*, Vol. 105, No. 1052, 2001, pp. 557–570.

[11] Carré, M. J., James, D. M., and Haake, S. J., "Impact of a Non-Homogeneous Sphere on a Rigid Surface," *Proceedings of the Institution of Mechanical Engineers Part C, Mechanical Engineering Science*, Vol. 218, No. 3, 2004, pp. 273–281. doi:10.1243/095440604322900408

[12] Stronge, W. J., and Ashcroft, A. D.C., "Oblique Impact of Inflated Balls at Large Deflections," *International Journal of Impact Engineering*, Vol. 34, No. 6, 2007, pp. 1003–1019. doi:10.1016/j.ijimpeng.2006.04.006

[13] Moys, M. H., and Dong, H., "Measurement of Impact Behaviour Between Balls and Walls in Grinding Mills," *Minerals Engineering*, Vol. 16, No. 6, 2003, pp. 543–550. doi:10.1016/S0892-6875(03)00057-8

[14] Jackson, P. (ed.), *Jane's All the World's Aircraft 2007–2008*, Jane's Information Group, London, 2007.

[15] "Aircraft Tire Care and Maintenance," Goodyear Tire & Rubber Co., Publ. 700-862-931-538, Akron, OH, 2004.

[16] Parker, G. W., "Projectile Motion with Air Resistance Quadratic in the Speed," *American Journal of Physics*, Vol. 45, No. 7, 1977, pp. 606–610. doi:10.1119/1.10812

[17] Watts, R. G., and Ferrer, R., "The Lateral Force on a Spinning Sphere: Aerodynamics of a Curveball," *American Journal of Physics*, Vol. 55, No. 1, 1987, pp. 40–44. doi:10.1119/1.14969

[18] Olsson, R., Donadon, M. V., and Falzon, B. G., "Delamination Threshold Load for Dynamic Impact on Plates," *International Journal of Solids and Structures*, Vol. 43, No. 10, 2006, pp. 3124–3141. doi:10.1016/j.ijsolstr.2005.05.005